EPR of Co^{2+}-doped $NiSO_4 \cdot 7H_2O$ and $MgSO_4 \cdot 7H_2O$: Co^{2+}-Ni^{2+} exchange interaction

Sushil K. Misra, Changlu Wang,* Shiying Han,† and Stefan Z. Korczak‡
Physics Department, Concordia University, 1455 de Maisonneuve Boulevard West, Montreal, Quebec, Canada H3G 1M8
(Received 2 February 1987)

X-band EPR measurements on Co^{2+}-doped isostructural single crystals of paramagnetic host $NiSO_4 \cdot 7H_2O$ and diamagnetic host $MgSO_4 \cdot 7H_2O$ have been made at liquid-helium temperature. The principal values of the $\vec{\vec{g}}^2$ and $\vec{\vec{A}}^2$ tensors, as well as the orientations of the principal axes of the $\vec{\vec{g}}^2$ and $\vec{\vec{A}}^2$ tensors, are evaluated from the data using a rigorous least-squares-fitting program suitable for electron-nuclear spin-coupled systems. Using the *g* shift of Co^{2+} in the paramagnetic lattice from that in the diamagnetic lattice the value of -0.81 GHz for the average Co^{2+}-Ni^{2+} exchange constant in $NiSO_4 \cdot 7H_2O$ has been estimated using the molecular-field approximation.

I. INTRODUCTION

The present paper reports, for the first time, *X*-band EPR studies on Co^{2+}-doped isomorphic single crystals of paramagnetic nickel sulphate heptahydrate $NiSO_4 \cdot 7H_2O$ (hereafter NSO) and diamagnetic magnesium sulphate heptahydrate $MgSO_4 \cdot 7H_2O$ (hereafter MSO) at liquid-helium temperature. Particular emphasis will be placed on the estimation of the paramagnetic-guest–paramagnetic-host (Co^{2+}-Ni^{2+}) exchange interaction using the shift of the *g* value of Co^{2+} in the paramagnetic host (NSO) from that in the isostructural diamagnetic host (MSO).

It is well known that the EPR spectrum of Co^{2+} ions cannot be observed at room temperature, since the spin-lattice relaxation time of Co^{2+} is very short at room temperature. It can only be observed at low temperatures. Thus, it is not possible to orient the crystal at room temperature so that the principal planes of the $\vec{\vec{g}}^2$ tensor are coincident with the planes in which the external magnetic field can be oriented. In the present apparatus the crystal could not be rotated at low temperatures around two mutually perpendicular axes. Thus, the plane in which the magnetic field can be rotated cannot, in general, be made to coincide with the principal planes of the $\vec{\vec{g}}^2$ tensor at liquid-helium temperature. On the other hand, by applying the least-squares procedure, fitting simultaneously a large number of resonant EPR line positions, obtained for a large number of external magnetic field orientations in any three mutually perpendicular planes, very accurate values of the elements of the $\vec{\vec{g}}^2$ and $\vec{\vec{A}}^2$ tensors can be obtained. From these the principal values, as well as the direction cosines of the principal axes, of the $\vec{\vec{g}}^2$ and $\vec{\vec{A}}^2$ tensors can be obtained.[1] From the principal values of the $\vec{\vec{g}}^2$ tensor the shift of the *g* value of Co^{2+} in the NSO host from that in the MSO host can be calculated; this is required to estimate the Co^{2+}-Ni^{2+} exchange constant in the NSO host. This study is similar to that already reported to estimate the Mn^{2+}-Fe^{2+}, Mn^{2+}-Ni^{2+}, and the Gd^{3+}-Yb^{3+} exchange interactions.[2–7]

II. *g* SHIFT

At liquid-helium temperature Δg, the shift of Co^{2+} *g* value in the paramagnetic lattice of Ni^{2+} in NSO from that in the isostructural diamagnetic lattice of Mg^{2+} in MSO originates from two effects: (i) The presence of an additional internal demagnetization magnetic field over and above the external magnetic field at the Co^{2+} site because of the polarization of the magnetic moments of the paramagnetic host ions Ni^{2+} produced by the external magnetic field. This demagnetization field depends on the shape of the sample, being zero for a spherical sample.[8] Thus, if one were to choose a spherical sample, as was done in the present case, the *g* shift at low temperature would solely be due to the guest-host (Co^{2+}-Ni^{2+}) exchange interaction. (ii) The exchange interaction between the host (Ni^{2+}) and probe (Co^{2+}) paramagnetic ions. This can be taken into account using the molecular-field approximation as follows.

Considering the nearest-neighbor Ni^{2+} host ions only, the spin Hamiltonian of a Co^{2+}-Ni^{2+} pair can be expressed as

$$\mathcal{H}_T = \mathcal{H} + \mathcal{H}' + \mathcal{H}_p \ . \tag{2.1}$$

In Eq. (2.1),

$$\mathcal{H} = \mu_B \mathbf{S} \cdot \vec{\vec{g}} \cdot \mathbf{H} \tag{2.2}$$

is the spin Hamiltonian of Co^{2+} ion ($S = \frac{1}{2}$), neglecting the hyperfine interaction; here $\vec{\vec{g}}$ is the $\vec{\vec{g}}$ tensor for Co^{2+} and μ_B is the Bohr magneton. (See Sec. V for more details.) Also,

$$\mathcal{H}' = \mu_B \mathbf{S} \cdot \vec{\vec{g}}_1 \cdot \mathbf{H} + 3\beta_2^0 O_2^0 + \beta_2^2 O_2^2 \ , \tag{2.3}$$

is the spin Hamiltonian of the Ni^{2+} ion ($S = 1$), where $\vec{\vec{g}}_1$ is the $\vec{\vec{g}}$ tensor of Ni^{2+}, and O_l^m are spin operators for $S = 1$ as defined by Abragam and Bleaney,[9] and

$$\mathcal{H}_p = J \mathbf{S} \cdot \mathbf{S}_1 \ , \tag{2.4}$$

represents the Co^{2+}-Ni^{2+} pair exchange interaction. Here *J* is the Co^{2+}-Ni^{2+} exchange interaction constant.

St. John and Myers have calculated the *g* shift of guest ions (Mn^{2+}) in paramagnetic hosts using the molecular-field model as follows.[10,11] The *g* shift can be expressed as

$$\Delta g = zJ \left\langle \frac{\partial E_n}{\partial H} \right\rangle \Big/ (g_1 \mu_B^2 H) \ . \tag{2.5}$$

In Eq. (2.5), z is the number of equivalent nearest and next-nearest neighbors and $\langle \partial E_n / \partial H \rangle$ is the average of the derivative over the lowest-lying triplet of the host ions. Finally, using the expression for E_n as given by Griffiths and Owen,[12] the average exchange interaction can be expressed as (see the Appendix)

$$J = (g^p_{z'z'} - g^d_{z'z'})[(\beta_2^2)^2 + (g_1 \mu_B H)^2]^{1/2} / 6 g_1 (P_2 - P_1) , \tag{2.6}$$

where the factor 6 appearing in the denominator represents the number of nearest and next-nearest host neighbors Ni^{2+} to a Co^{2+} ion, $g^p_{z'z'}$ and $g^d_{z'z'}$ are the principal g values of Co^{2+} as observed in the paramagnetic host (NSO) and diamagnetic host (MSO), respectively, and P_1 and P_2 are the probabilities of Ni^{2+} ions of being in the lowest and the next-lowest levels of the ground-state triplet, respectively. $g_1 = 2.25$ and $|\beta_2^2| = 45$ GHz as determined by Ono[13] for NSO, and an average value of H can be used to be 3500 G, typical of X-band spectrum.

III. CRYSTAL STRUCTURE AND SAMPLE PREPARATION

The MSO and NSO crystals are isomorphic, each characterized by an orthorhombic unit cell. The unit cell contains four formula units related to each other by the space-group operator $P_{2_12_12_1}$. The unit-cell dimensions are, for NSO: $a = 11.86$ Å, $b = 12.08$ Å, $c = 6.81$ Å; and for MSO: $a = 11.91$ Å, $b = 12.02$ Å, $c = 6.87$ Å. In these crystals each Ni^{2+}, or Mg^{2+}, ion is surrounded by a distorted octahedron of six water molecules. The seventh water molecule, not coordinated with a Ni^{2+} or Mg^{2+} ion, instead fills what would otherwise be a hole in the structure.[14] The four Ni^{2+} or Mg^{2+} sites in the unit cell are physically inequivalent, but magnetically equivalent; this is reflected in the EPR spectra.

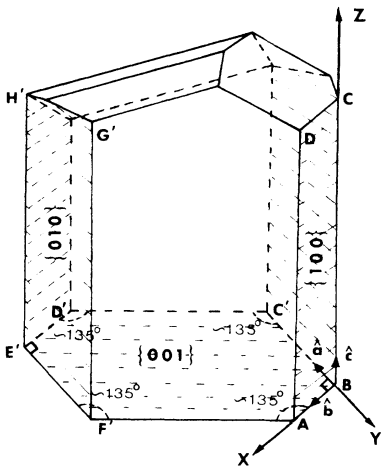

FIG. 1. The crystal growth habit of MSO crystal used for the EPR measurements. The orientations of the EPR axes X, Y, and Z (laboratory frame) with respect to the crystal faces have been indicated. $ABCD$, $ABC'D'E'F'$, and $E'F'G'H'$ are, respectively, $\{100\}$, $\{001\}$, and $\{010\}$ planes. The directions of unit vectors $\hat{\mathbf{a}}$, $\hat{\mathbf{b}}$, $\hat{\mathbf{c}}$ along the unit-cell vectors **a**, **b**, **c** are indicated.

Single crystals of Co^{2+}-doped NSO and MSO were grown by slow evaporation, at room temperature, of the respective saturated solutions, each containing 1 mol% $CoSO_4 \cdot 7H_2O$. The crystals were protected against moisture by dipping them in mineral oil. The growth habits of the two crystals are the same; they are exhibited in Fig. 1.

IV. EXPERIMENTAL DETAILS

A VARIAN V4502 X-band spectrometer was used for the present observations. The magnetic field measurements were made with a Bruker (B-NM20) gaussmeter. For angular variation studies at liquid-helium temperature, the crystal was kept fixed while the magnetic field was rotated. The temperature was varied by the use of a heater resistor, installed in the liquid-helium cryostat. A spherial sample of Co^{2+}-doped NSO was prepared by rubbing a sufficiently large single crystal on a damp filter paper. EPR spectra were recorded in three arbitrary mutually perpendicular planes, defined by the axes X, Y, Z, for the magnetic field orientations at 2° intervals. The ZX plane was chosen parallel to a crystal face; the orientation of the Z and X axes are exhibited in Fig. 1. Specifically, the Z axis was chosen parallel to the c axis while the X axis was chosen parallel to the b axis, being guided by the crystal faces (Fig. 1).

Co^{2+} EPR lines were clearly observed at 4.2 K. The similarity of the EPR spectra of the two samples, except for a little difference in the linewidths and intensities, caused by the presence of the paramagnetic Ni^{2+} ions in the NSO lattice, confirmed that the MSO and NSO crystals were, indeed, isostructural.

The angular variation of the spectra for rotation of the external magnetic field in any plane revealed the presence of four different sets of eight allowed Co^{2+} hyperfine lines $\Delta M = \pm 1$, $\Delta m = 0$, where M and m are, respectively, the electronic and nuclear quantum numbers. These correspond to the four physically inequivalent sites in the unit cell, which Co^{2+} ions can occupy. Except for the difference in the orientations of the respective principal axes, these four sets of spectra are found to be identical in all respects. The angular variations of the spectra for the MSO host in the ZX, ZY, and XY planes at liquid-helium temperature are displayed in Figs. 2, 3, and 4, respectively.

The peak-to-peak linewidth of the first-derivative absorption line shape for the NSO host, as a function of temperature, is exhibited in Fig. 5. It is found that upon raising the temperature, the linewidths increased, while the intensities decreased. Finally, at about 47 K the lines disappeared completely in both the MSO and NSO hosts. It should be noted that at 4.2 K the average linewidths in MSO and NSO hosts are 39 and 30 G, respectively. The linewidths in the two hosts are, in general, not very different from each other. As well, they are independent of the orientation of the external magnetic field.

No EPR spectra due to Ni^{2+} could be observed in the NSO host. This can be explained as follows. The lowest

level (ground state) of the even-electron $3d^8$ (^3F) configuration of Ni^{2+} is an orbital singlet in an octahedral field; it has threefold spin degeneracy. A field of orthorhombic, or lower, symmetry removes both the orbital and spin degeneracies of its ground state completely. The splitting of the ground-state triplet between adjacent levels in the absence of a magnetic field are $|3\beta_2^0-\beta_2^2|$ and $2|\beta_2^2|$, where $|3\beta_2^0|$ and $|\beta_2^2|$ are the fine-structure constants of Ni^{2+} defined by Eq. (2.3). The values of these parameters are $3\beta_2^0=-106.8$ GHz and $\beta_2^2=-45$ GHz for NSO.[13] This splitting is much larger than the X-band microwave quantum (~ 9.5 GHz); thus the EPR of Ni^{2+} cannot be observed at X-band frequencies.[15]

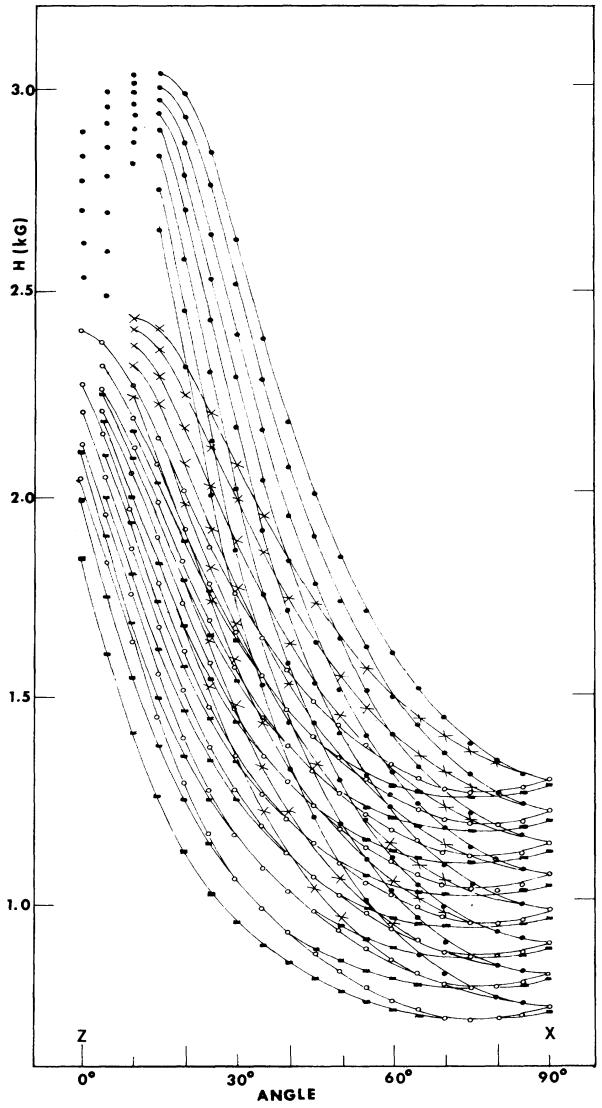

FIG. 2. Angular variation of the X-band spectra in the ZX plane for Co^{2+}-doped MSO. The circles, solid rectangles, solid circles, and crosses represent the experimental line positions of the four physically inequivalent Co^{2+} complexes. The solid lines are smooth curves that connect data points for the same transition. The spin Hamiltonian parameters have been estimated using the line positions represented by circles.

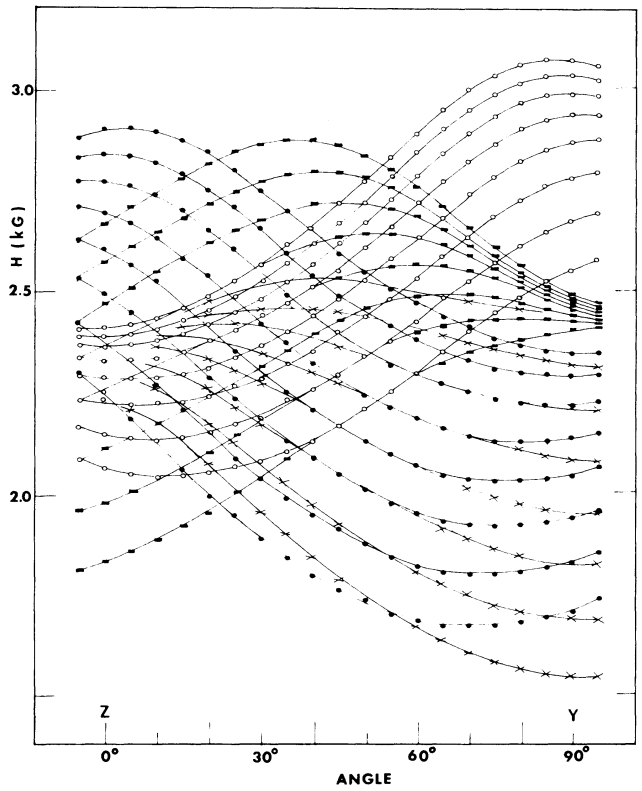

FIG. 3. Angular variation of the X-band spectra in the ZY plane for Co^{2+}-doped MSO. Further details are the same as those expressed in the caption of Fig. 2.

V. SPIN HAMILTONIAN AND EVALUATION OF PARAMETERS

The ground state ^4F of Co^{2+} ($3d^7$ configuration) is split by an octahedral field, such that an orbital triplet lies lowest, which further splits into Kramers doublets under the combined effect of the spin-orbit coupling and fields of lower symmetry. The external magnetic field removes the Kramers degeneracy. The separation between the lowest-lying Kramers doublet and the next-higher level is much larger than the X-band microwave quantum. Thus, the Co^{2+} ion has an effective electron spin $S=\frac{1}{2}$ in the MSO, or in the NSO, host, since it is only the lowest-lying Kramers doublet which participates in EPR. In addition, the cobalt ion has a nuclear spin $I=\frac{7}{2}$. Finally, the spin Hamiltonian for Co^{2+} in these hosts can be written as[16]

$$\mathcal{H}=\mu_B\mathbf{H}\cdot\overleftrightarrow{g}\cdot\mathbf{S}+\mathbf{S}\cdot\overleftrightarrow{A}\cdot\mathbf{I}+\mathbf{I}\cdot\overleftrightarrow{Q}\cdot\mathbf{I}\ . \tag{4.1}$$

In Eq. (4.1), $\overleftrightarrow{A}$ and $\overleftrightarrow{Q}$ are the hyperfine and nuclear quadrupole tensors, respectively, for the Co^{2+} ion.

The parameters were evaluated by the use of a rigorous least-squares-fitting (LSF) method, employing exact numerical diagonalization of the spin-Hamiltonian

matrix, as described in Ref. 1. The elements of the tensor $\vec{Q}$ could not be determined from the allowed line positions, since the corresponding energy differences do not depend upon them. The estimated fine-line positions (60 in total) corresponding to the set of eight hyperfine line positions for the magnetic field orientation in the three mutually perpendicular planes for one physically inequivalent Co^{2+} ion, as estimated assuming the hyperfine interaction to be zero, were first fitted simultaneously to evaluate the components of the $\vec{g}^2$ tensor by a LSF procedure.[1] The matrix of the $\vec{g}^2$ tensor, so obtained, was then diagonalized to obtain the principal values of the $\vec{g}^2$ tensor (which are squares of the principal values of the $\underline{g}$ matrix), and the direction cosines of its principal axes (same as those of the $\underline{g}$ matrix). Table I lists the principal g values and the direction cosines of the principal

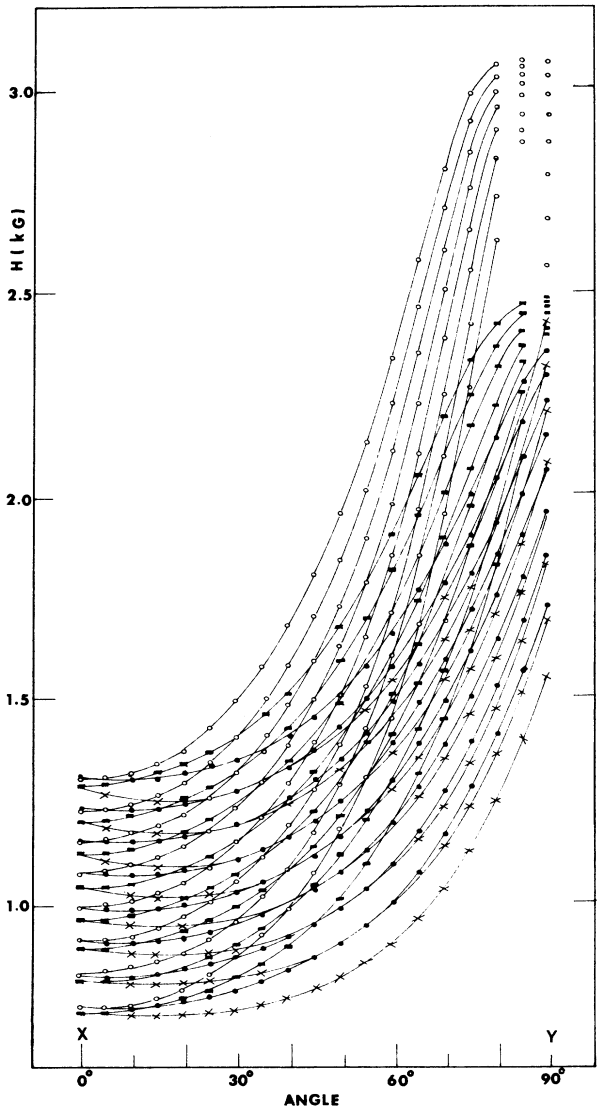

FIG. 4. Angular variation of the X-band spectra in XY plane for Co^{2+}-doped MSO. Further details are the same as those expressed in the caption of Fig. 2.

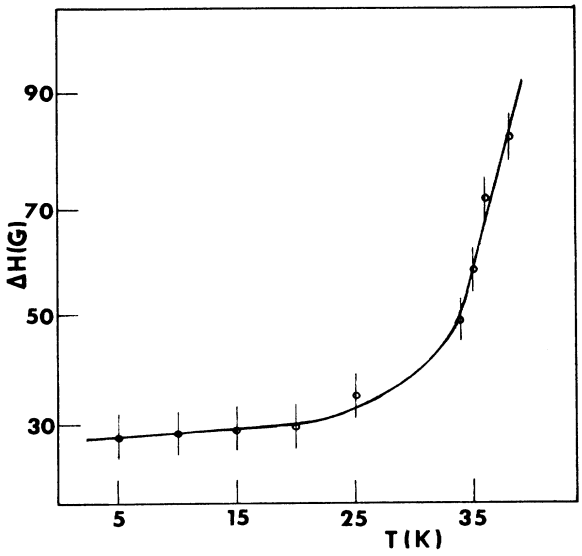

FIG. 5. Variation of the average linewidth as a function of temperature for the direction of the external magnetic field along the X axis for NSO host.

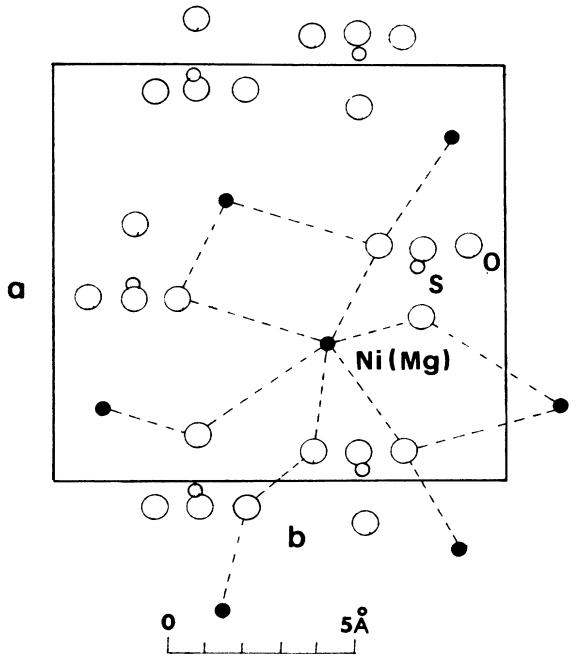

FIG. 6. Partial projection of the NSO unit-cell structure on to {001} plane showing six nearest and next-nearest neighbors Ni^{2+} ions (large solid circles) and six SO_4^{2-} groups. Small open circles represent sulphurs, while large open circles represent oxygens. The lengths a and b are the unit-cell dimensions. The indirect exchange between Co^{2+} and Ni^{2+} ions is dominantly via $2s$ and $2p$ orbitals of one or two oxygen ions. Examples of such exchange paths have been shown by dotted lines.

TABLE I. Principal values and the direction cosines of the principal axes of the $\underline{g}$ and $\underline{A}$ matrices of Co^{2+}-doped NSO and MSO hosts at 4.2 K. g is dimensionless, while A is expressed in units of GHz. The indicated errors are as estimated by the use of a statistical method (Ref. 17). The direction cosines of the $\vec{\vec{g}}^2$ tensor are given with respect to the X, Y, Z axes (laboratory frame), defined in Sec. IV and depicted in Fig. 1, while those of the $\vec{\vec{A}}^2$ tensor (X'', Y'', Z'') are expressed relative to (X', Y', Z'), the principal axes of the $\vec{\vec{g}}^2$ tensor.

Host		Principal values			Direction cosines Z	X	Y
NSO	$g_{z'z'}$	7.100	0.009	Z'	0.074	0.981	0.182
	$g_{x'x'}$	2.936	0.004	X'	−0.991	0.053	0.121
	$g_{y'y'}$	2.320	0.003	Y'	0.109	−0.189	0.976

Host		Principal values			Direction cosines Z'	X'	Y'
NSO	$A_{z''z''}$	0.806	0.004	Z''	0.983	0.125	−0.137
	$A_{x''x''}$	0.303	0.002	X''	0.048	0.544	0.838
	$A_{y''y''}$	0.000	0.001	Y''	0.179	−0.830	0.529

Host		Principal values			Direction cosines Z	X	Y
MSO	$g_{z'z'}$	7.008	0.009	Z'	0.035	0.990	−0.140
	$g_{x'x'}$	2.928	0.002	X'	−0.998	0.026	−0.063
	$g_{y'y'}$	2.198	0.003	Y'	−0.057	0.142	0.988

Host		Principal values			Direction cosines Z'	X'	Y'
MSO	$A_{z''z''}$	0.765	0.004	Z''	0.997	0.070	0.036
	$A_{x''x''}$	0.246	0.001	X''	−0.059	0.966	−0.254
	$A_{y''y''}$	0.000	0.001	Y''	−0.052	0.251	0.967

axes of the $\vec{\vec{g}}^2$ tensor with respect to the X, Y, Z axes for the two hosts. In order to evaluate the elements of the $\vec{\vec{A}}^2$ tensor the previously determined principal $\vec{\vec{g}}^2$ values and their direction cosines were used in another LSF procedure, fitting simultaneously 384 allowed hyperfine transition line positions for the external magnetic field orientations in the three planes ZX, ZY, and XY of the same Co^{2+} complex for which the elements of the $\vec{\vec{g}}^2$ tensor were evaluated. The matrix corresponding to the tensor $\vec{\vec{A}}^2$ was then diagonalized to obtain the squares of the principal values of the $\vec{\vec{A}}^2$ tensor, as well as its direction cosines, with respect to the principal axes of the $\vec{\vec{g}}^2$ tensor. These values are also listed in Table I. The parameter errors were determined by the use of a statistical method.[17] Since the relationship of the X, Y, Z axes with respect to the crystal growth habit is known (Fig. 1), the direction cosines of the principal axes of the $\vec{\vec{g}}^2$ and $\vec{\vec{A}}^2$ matrices, thus, define completely the principal directions of the $\vec{\vec{g}}^2$ and $\vec{\vec{A}}^2$ matrices with respect to the crystal axes.

VI. Co^{2+}-Ni^{2+} EXCHANGE INTERACTION

Using expression (2.6) for J, as obtained from the molecular-field approximation, an average value of J was found to be −0.81 GHz. The exchange interaction J has been shown to depend on interatomic distance R, as R^{-12}.[18] It was later found that an exponential function $J = J_0 e^{-bR}$, with $b = 3.55$ worked better than the power law for a number of systems.[19] The exchange has also been expressed as a function of bond angles.[19] The paramagnetic shift[20] in the g value may be used to estimate the Co^{2+}-Ni^{2+} exchange interaction in NSO.[20] In the present paper it is assumed that the shift arises mainly from a total of six (nearest and next-nearest) neighbors, as the factor $\exp(-bR)$ gives rise to a considerable reduction of J at distances increased by 20%. Furthermore, the magnitude of the crystal-field splittings, 61.8 and 90.0 GHz, is much larger than that of $J = -0.81$ GHz. Thus the g shift is so small that it only provides an approximate estimate of the exchange interaction. It is of interest to visualize the exchange path in NSO. The exchange is an indirect exchange interaction through one ion of O^{2-} (Co^{2+}-O^{2-}-Ni^{2+}) or two ions of O^{2-} (Co^{2+}-O^{2-}-O^{2-}-Ni^{2+}), which belong to SO_4^{2-} ions, as shown in Fig. 6 on the basis of the crystal structure data, reported by Wyckoff.[14] The ligand-ligand overlap is also important in the exchange interaction in the present systems.

ACKNOWLEDGMENTS

The authors are grateful to the Natural Sciences and Engineering Research Council of Canada for financial support (Grant No. A4485), and to the Concordia University Computer Center for providing their facilities to analyze the data.

APPENDIX

The average of the derivative of energy with respect to magnetic field of the lowest-lying triplet of Ni^{2+} can be expressed as

$$\left\langle \frac{\partial E_n}{\partial H} \right\rangle = \sum_{i=1}^{3} \frac{\partial E_i}{\partial H} P_i \ ,$$

where E_1, E_2, and E_3 are the energies of the ground-state triplet in increasing values, and P_1, P_2, and P_3 are the corresponding probabilities of occupation of these states. According to Griffiths and Owen,[12] for $\mathbf{H} \| \hat{\mathbf{z}}$ these energies are

$$E_1 = 3\beta_2^0 - [(\beta_2^2)^2 + (g_1 \mu_B H)^2]^{1/2} \ , \tag{A1}$$

$$E_2 = 3\beta_2^0 + [(\beta_2^2)^2 + (g_1 \mu_B H)^2]^{1/2} \ , \tag{A2}$$

and

$$E_3 = 0 \ . \tag{A3}$$

Thus

$$\left\langle \frac{\partial E_n}{\partial H} \right\rangle = [(\beta_2^2)^2 + (g_1 \mu_B H)^2]^{-1/2} (P_2 - P_1) g_1^2 \mu_B^2 H \ , \tag{A4}$$

to be used in Eq. (2.5).

Finally, the probabilities P_i can be expressed as

$$P_i = \exp(-E_i/kT) \Big/ \sum_{i=1}^{3} \exp(-E_i/kT) \ , \tag{A5}$$

where E_i are as given by Eqs. (A1)–(A3). The required values of the parameters are[13] $3\beta_2^0 = -106.8$ GHz and $\beta_2^2 = -45$ GHz, while $T = 4.2$ K for the present data. This yields $P_1 = 0.648$, $P_2 = 0.253$, and $P_3 = 0.099$.

---

*On leave of absence from the Physics Department, Jilin University, Jilin, China.

†Permanent address: Centre of Materials Analysis, Nanjing University, Nanjing, China.

‡Permanent address: Department of Experimental Physics, Maria Curie Sklodowska University, 20-031 Lubin, Poland.

[1]S. K. Misra, Physica **124B**, 53 (1983); application illustrated in S. K. Misra, G. Bandet, G. Bacquet, and T. E. McEnally, Phys. Status Solidi A **80**, 581 (1983).

[2]S. K. Misra and S. Z. Korczak, Phys. Rev. B **34**, 3086 (1986).

[3]S. K. Misra and M. Kahrizi, Phys. Rev. B **28**, 5300 (1983).

[4]S. K. Misra and M. Kahrizi, Phys. Rev. B **30**, 2920 (1984).

[5]S. K. Misra and M. Kahrizi, Phys. Rev. B **30**, 5352 (1984).

[6]S. K. Misra, M. Kahrizi, P. Mikolajczak, and L. Misiak, Phys. Rev. B **32**, 4738 (1985).

[7]S. K. Misra and S. Z. Korczak, Phys. Rev. B **35**, 4625 (1986).

[8]C. Kittel, Phys. Rev. **73**, 155 (1948).

[9]A. Abragam and B. Bleaney, *Electron Paramagnetic Resonance of Transition Ions* (Clarendon, Oxford, 1970).

[10]M. R. St. John and R. J. Myers, Phys. Rev. B **13**, 1006 (1975).

[11]S. K. Misra and M. Kahrizi (unpublished).

[12]J. H. E. Griffiths and J. Owen, Proc. R. Soc. London, Ser. A **213**, 459 (1952).

[13]K. Ono, J. Phys. Soc. Jpn. **8**, 802 (1953).

[14]R. W. G. Wyckoff, *Crystal Structure* (Interscience, New York, 1965), Vol. 3, p. 837.

[15]R. Janakiraman and G. C. Upreti, J. Chem. Phys. **54**, 2336 (1971).

[16]P. Chand and G. C. Upreti, J. Chem. Phys. **86**, 15 (1985).

[17]S. K. Misra and S. Subramanian, J. Phys. C **15**, 7199 (1982).

[18]K. N. Shrivastava and V. Jaccarino, Phys. Rev. B **13**, 299 (1976).

[19]K. N. Shrivastava, Phys. Status Solidi B **125**, 11 (1984); **125**, 441 (1984).

[20]M. T. Hutchings, C. G. Windsor, and W. P. Wolf, Phys. Rev. **148**, 444 (1966); R. J. Birgeneau, M. T. Hutchings, and W. P. Wolf, *ibid.* **179**, 275 (1969).